Eur. Phys. J. C 13, 681–690 (2000)
Digital Object Identifier (DOI) 10.1007/s100520000258

THE EUROPEAN PHYSICAL JOURNAL C

Topologies of the (M+1)SSM with a singlino LSP at LEP2

U. Ellwanger, C. Hugonie

Laboratoire de Physique Théorique et Hautes Energies[a], Université de Paris XI, Centre d'Orsay, 91405 Orsay Cedex, France

Received: 15 January 1999 / Revised version: 20 May 1999 /
Published online: 17 March 2000 – © Springer-Verlag 2000

Abstract. We study the possible signals of the (M+1)SSM with a singlino LSP at LEP2. First we identify regions of the parameter space which are ruled out by negative results of sparticle searches in the context of the MSSM. In the remaining kinematically accessible regions we present total event rates for topologies which require further studies, i.e. estimations of the corresponding efficiencies: various four charged fermion final states with missing energy, possibly with displaced vertices due to a long life time of the NLSP, the second lightest neutralino. Searches for these unconventional signatures are essential in order to cover the entire kinematically accessible parameter space of the (M+1)SSM with a singlino LSP at LEP2.

1 Introduction

The supersymmetric extension of the standard model with an additional gauge singlet superfield, the so-called (M+1)SSM [6,1,5,4,8,9,2,10,7], naturally solves the μ-problem of the MSSM: Even for a scale invariant superpotential – with a coupling $\lambda S H_1 H_2$ among the Higgs superfields and the singlet superfield S – an effective μ-term $\mu = \lambda \langle S \rangle$ is generated, if the scalar component of S has a non-vanishing VEV. Such a VEV of the order of the weak scale can be generated through the standard soft supersymmetry breaking terms; thus the weak scale appears exclusively in the form of the supersymmetry breaking scale. Moreover, assuming universal soft terms at a large (GUT) scale, the (M+1)SSM has the same number of free parameters as the MSSM. Previous analyses of the parameter space of the model [5–7] have shown that, as in the case of the MSSM, a large region is consistent with the present experimental bounds on sparticle and Higgs masses.

The particle content of the (M+1)SSM differs from the MSSM in the form of additional gauge singlet states in the Higgs sector (1 neutral CP-even and 1 CP-odd state) and in the neutralino sector (a two component Weyl fermion). These states mix with the corresponding ones of the MSSM, with a mixing angle which is proportional to the coupling λ above. Accordingly, the phenomenology of the (M+1)SSM depends on to large extent on the magnitude of λ.

For $\lambda \gtrsim O(10^{-2})$ the masses and couplings, notably in the CP-even Higgs sector, can deviate visibly from the ones of the MSSM [4]; however, in this region of the parameter space of the (M+1)SSM some fine tuning among the parameters is required in order to meet all the phenomenological constraints [6].

For $\lambda \lesssim O(10^{-2})$ the mixing angles involving the singlet states are quite small. Therefore, the Higgs and sparticle masses and couplings of the (M+1)SSM are very close to the MSSM ones (for corresponding values of μ and B [5, 6]), with additional quasi-singlet states which have small couplings to the gauge bosons and the MSSM sparticles. Accordingly, they have small production cross sections, and they will not appear in sparticle decays unless they represent the only kinematically allowed decay channel.

Assuming R-parity conservation, this latter situation is realized if the quasi-singlet Weyl fermion (the singlino) is the LSP. Then the singlino will appear in the final state of each sparticle decay, and the phenomenology of the (M+1)SSM with a singlino LSP differs considerably from the one of the MSSM.

In a previous paper [7] we have shown that this situation appears naturally in the case of a gaugino dominated supersymmetry breaking: $M_{1/2} \gg A_0, m_0$. Then, within the parameter space accessible at LEP2, the NLSP is mostly a bino-like state. Hence all the processes involving sparticle productions and decays will end up with a bino to singlino transition, and we have studied the corresponding decay widths in [7]. An important result was that, for small values of λ or for singlino masses close to the bino mass, the bino life time can be so large that the bino to singlino cascade appears at macroscopic distances from the production point, or even out of the detector.

In the present paper we study the possible signals of the (M+1)SSM with a singlino LSP at LEP2 in the various regions of the parameter space. First we identify those regions which are ruled out by negative results of sparticle searches in the context of the MSSM. In the remaining kinematically allowed regions we present total event rates for various topologies, like four charged fermion fi-

[a] Laboratoire associé au Centre National de la Recherche Scientifique (URA D0063)

nal states and missing energy, with or without displaced vertices. Such topologies, with microscopic vertices, have been looked for at LEP2 in the context of the MSSM or models with R-parity violation. However the corresponding efficiencies do not apply to the (M+1)SSM with a singlino LSP. With the estimated efficiencies, we find that considerable kinematically allowed regions of the parameter space have not been tested at present, especially in the case of macroscopically displaced vertices. The main purpose of the present paper is to identify those topologies, for which further studies – i.e. estimation of the efficiencies – are required in order to interpret the available or incoming data from LEP2 in the context of the (M+1)SSM with a singlino LSP.

It is a priori not clear whether negative results of sparticle searches would constrain the (M+1)SSM with a singlino LSP more or less than the MSSM: The final states associated with the pair production of a given sparticle (like the selectron or chargino) will often be more involved in the (M+1)SSM as compared to the MSSM, and the corresponding constraints on the cross sections are often much weaker. On the other hand, the (M+1)SSM with a singlino LSP allows for a process to be observable which is invisible within the MSSM: the production of a pair of binos. If the binos decay into singlinos plus additional observable particles, LEP2 is sensitive to light binos which would, however, escape detection within the associated MSSM. (Here and below the associated MSSM denotes the MSSM obtained after "freezing" the singlet VEV, which generates effective μ- and B-terms, and after dropping the gauge singlet states in the neutralino and Higgs sectors.) Thus the application of the LEP2 results to the (M+1)SSM requires a case by case analysis, depending on the different regions of the parameter space. This will be performed below.

In order to scan the complete parameter space of the (M+1)SSM we proceed as in [6,7]: First we assume universal scalar masses m_0, gaugino masses $M_{1/2}$ and trilinear couplings A_0 at the GUT scale. Thus we scan over the ratios $m_0/M_{1/2}$, $A_0/M_{1/2}$ and the Yukawa couplings at the GUT scale, the absolute scale being determined in the end by requiring the correct value of M_Z. For each point in the parameter space we integrate the renormalization group equations [2] down to the weak scale, and minimize the low energy effective potential including the full one loop radiative corrections [4]. We check whether squarks or sleptons do not assume VEVs, diagonalize numerically the mass matrices and verify whether applicable bounds on sparticle and Higgs masses are satisfied.

In contrast to [6,7], however, we have included as matter Yukawa couplings not just the top Yukawa coupling h_t, but all the couplings of the third generation h_t, h_b and h_τ. First, this makes our results more reliable in the large $\tan(\beta)$ regime, and second this reveals a new phenomenon: Within the (M+1)SSM with a singlino LSP and sparticle masses in the reach of LEP2, the NLSP could possibly be the lightest stau $\widetilde{\tau}_1$. (In the associated MSSM the lightest stau $\widetilde{\tau}_1$ would then be the true LSP, i.e. a stable charged particle; this situation has been discussed in [11].)

The paper is organized as follows: In Sect. 2 we present the lagrangian and discuss the different regions in the parameter space which are relevant for the present investigations. In Sect. 3 we study the sparticle production processes which are kinematically allowed at LEP2, the topologies relevant for searches in the context of the (M+1)SSM with a singlino LSP, and the constraints on its parameters which could be already infered from available data. The total number of events expected in those regions of parameter space is given, for which the efficiencies still remain to be determined. Conclusions are presented in Sect. 4.

2 Parameter space of the (M+1)SSM with a singlino LSP

The superpotential of the (M+1)SSM is given by

$$W = \lambda S H_1 H_2 + \frac{1}{3}\kappa S^3 + h_t Q_3 H_1 U^c_{3R} + h_b Q_3 H_2 D^c_{3R} + h_\tau L_3 H_2 E^c_{3R} + \ldots, \qquad (1)$$

where Q_3 denotes the left handed doublet of quarks of the third generation, $U^c_{3\mathrm{R}}$ and $D^c_{3\mathrm{R}}$ the (charge conjugate) right handed top and bottom quarks, L_3 the left handed doublet of leptons of the third generation, $E^c_{3\mathrm{R}}$ the (charge conjugate) right handed tau. The ellipses in (1) denote Yukawa couplings involving quarks and leptons of the first two generations. The only dimensionful parameters of the model are the supersymmetry breaking parameters (for simplicity, we do not display the terms involving squarks and sleptons)

$$\mathcal{L}_{soft} = \frac{1}{2}\left(M_3 \lambda_3^a \lambda_3^a + M_2 \lambda_2^i \lambda_2^i + M_1 \lambda_1 \lambda_1\right) + \mathrm{h.c.} - m_1^2 |H_1|^2 - m_2^2 |H_2|^2 - m_S^2 |S|^2 - \lambda A_\lambda S H_1 H_2 - \frac{1}{3}\kappa A_\kappa S^3 + \mathrm{h.c.}, \qquad (2)$$

where λ_3, λ_2 and λ_1 (the "bino") are the gauginos of the $SU(3)_c$, $SU(2)_{\mathrm{L}}$ and $U(1)_Y$ gauge groups, respectively. The scalar components of the Higgs in (2) are denoted by the same letters as the corresponding chiral superfields. These supersymmetry breaking terms are constrained in the present version of the model by universality at the scale $M_{\mathrm{GUT}} \sim 10^{16}\,\mathrm{GeV}$. Thus, the independent parameters are: universal gaugino masses $M_{1/2}$ (always positive in our convention); universal masses m_0^2 for the scalars; universal trilinear couplings A_0 (either positive or negative); the Yukawa couplings h_{t0}, h_{b0}, $h_{\tau 0}$, and λ_0, κ_0 of the superpotential (1) at the scale M_{GUT}.

The parameters at the weak scale are obtained by numerically integrating the one loop renormalization group equations [2]. The Coleman–Weinberg radiative corrections to the effective potential involving top/stop, bottom/sbottom and tau/stau loops (beyond the leading log approximation) [4] are taken into account. The results for the mass matrices, after minimization of the effective potential, can be found in [1,2,4–7] and will not be repeated

here. Mixing terms are considered in the stop, sbottom and stau mass matrices.

Let us now discuss the parameter space of the (M+1)SSM with a singlino LSP which is relevant for sparticle searches at LEP2. Since here the Yukawa couplings λ and κ are quite small ($\lambda, \kappa \lesssim O(10^{-2})$) and hence the singlet sector mixes only weakly to the non-singlet sector, it is possible to understand the gross features of the parameter space with the help of analytic approximations to the integrated renormalization group equations, the minimization of the effective potential and the mass matrices [3,5–7]. (The results in Sect. 3, on the other hand, are based on "exact" numerical computations for $\sim 10^4$ points in the parameter space.)

First, we consider the neutralino sector. In our convention, the (symmetric) neutralino mass matrix is given by [12]

$$M^0 = \begin{pmatrix} M_2 & 0 & \frac{-g_2 h_1}{\sqrt{2}} & \frac{g_2 h_2}{\sqrt{2}} & 0 \\ & M_1 & \frac{g_1 h_1}{\sqrt{2}} & \frac{-g_1 h_2}{\sqrt{2}} & 0 \\ & & 0 & -\mu & -\lambda h_2 \\ & & & 0 & -\lambda h_1 \\ & & & & 2\kappa s \end{pmatrix}. \quad (3)$$

For small λ, the singlino is thus an almost pure state of mass

$$M_{\widetilde{S}} \simeq 2\kappa s. \quad (4)$$

and the VEV s of the scalar singlet can be estimated from the tree level scalar potential:

$$s \simeq -\frac{A_\kappa}{4\kappa}\left(1 + \sqrt{1 - \frac{8m_S^2}{A_\kappa^2}}\right). \quad (5)$$

Since A_κ and m_S are only slightly renormalized between $M_{\rm GUT}$ and the weak scale for small λ and κ, $M_{\widetilde{S}}$ can be written in terms of the universal soft terms at $M_{\rm GUT}$:

$$M_{\widetilde{S}} \simeq -\frac{A_0}{2}\left(1 + \sqrt{1 - \frac{8m_0^2}{A_0^2}}\right). \quad (6)$$

The condition for the minimum (5) to be deeper than the trivial one reads at tree level

$$|A_0| > 3m_0, \quad (7)$$

so that

$$\frac{2}{3}|A_0| \lesssim |M_{\widetilde{S}}| \lesssim |A_0|. \quad (8)$$

Since the effective μ parameter turns out to be quite large,

$$\mu^2 = \lambda^2 s^2 \simeq 2.5 M_{1/2}^2 - .5 M_Z^2, \quad (9)$$

the lightest non-singlet neutralino is the (nearly pure) bino $\widetilde{B}$ with mass $M_{\widetilde{B}}$. From the approximate analytic diagonalization of (3) for $\tan(\beta) \gtrsim 5$ (which, from our numerical results, is always the case for a singlino LSP), one obtains $M_{\widetilde{B}}$ in terms of the universal gaugino mass $M_{1/2}$ as

$$M_{\widetilde{B}} \simeq M_1 + \frac{\sin^2\theta_{\rm W} M_Z^2 M_1}{M_1^2 - \mu^2} \simeq 0.41 M_{1/2} - \frac{4.10^{-2} M_Z^2 M_{1/2}}{M_{1/2}^2 - 0.2 M_Z^2}, \quad (10)$$

where we have used (9) and $M_1 = 0.41 M_{1/2}$. The second term in (10) is due to the bino/higgsino mixing. From (6) and (10) one finds that the necessary (respectively sufficient) conditions on the universal terms for a singlino LSP are

$$|A_0| \lesssim 0.6 M_{1/2} \quad (\text{respectively } |A_0| \lesssim 0.4 M_{1/2}). \quad (11)$$

The Yukawa couplings λ and κ of the (M+1)SSM are, in general, constrained by the ratio $A_0/M_{1/2}$. From the absence of a deeper unphysical minimum of the Higgs potential with $h_2 = s = 0$ the following inequality can be derived:

$$\kappa \lesssim 4.10^{-2} \frac{A_0^2}{M_{1/2}^2}. \quad (12)$$

Since the singlet VEV s increases with decreasing κ (cf. (5)), but the effective μ-term should be of the order of the weak scale, λ and κ should be of the same order of magnitude. From our numerical analysis we find that the bare parameters A_0, $M_{1/2}$ and λ_0 satisfy the (not very stringent) relation

$$\frac{|A_0|}{M_{1/2}} \sim 4\lambda_0^{5\pm.3}; \quad (13)$$

thus light singlinos are generally related to small values of λ and κ. Since the mixing angle of the singlino to the non-singlet sector is proportional to λ, all decay widths of sparticles into a singlino LSP are at least proportional to λ^2. Furthermore, λ can be extremely small; then the NLSP life time is very large. This phenomenon, already investigated in [7], will play an important role in the next section.

Now we turn to the slepton sector. The lightest states are the "right handed" charged sleptons $\widetilde{l}_R$ and the sneutrinos $\widetilde{\nu}$. Since the bare scalar mass m_0 is quite small (cf. (7) and (11)) the corresponding mass terms at the weak scale are determined, from the integrated renormalization group equations, by $M_{1/2}$. Neglecting the mixing between the right handed and the left handed sleptons, and using the known numerical values of the electroweak gauge couplings appearing in the D-terms, their masses are (for medium or large $\tan(\beta)$)

$$m_{\widetilde{l}_R}^2 = m_E^2 - \sin^2\theta_{\rm W} M_Z^2 \cos 2\beta \simeq 0.15 M_0^2 + 0.23 M_Z^2, \quad (14)$$

$$m_{\widetilde{\nu}}^2 = m_L^2 + \tfrac{1}{2} M_Z^2 \cos 2\beta \simeq 0.52 M_0^2 - 0.5 M_Z^2. \quad (15)$$

The limit on the sneutrino mass obtained from the Z width, $m_{\widetilde{\nu}} \gtrsim M_Z/2$ [14], combined with (15) gives a lower limit on $M_{1/2}$:

$$M_{1/2} \gtrsim 100\,{\rm GeV}. \quad (16)$$

From (14) together with (10) it follows that the sleptons $\widetilde{l}_R$ are heavier than the bino for $M_{1/2} \lesssim 320\,\mathrm{GeV}$. However, this result holds only for the charged sleptons of the first two generations. For the third generation, the soft masses at low energy can be smaller than the ones given in (14) and (15) (depending on h_τ). Furthermore, the off-diagonal term in the stau mass matrix is given by $h_\tau(\mu h_1 - A_\tau h_2)$, which is not necessarily negligible compared to the smallest diagonal term. Thus, the lightest eigenstate $\widetilde{\tau}_1$ will be lighter than the right handed sleptons of the first two generations $\widetilde{l}_R$ and can well be lighter than the bino even for $M_{1/2} \lesssim 320\,\mathrm{GeV}$ (hence for sparticle masses within the reach of LEP2).

In the chargino sector, within the present region of the parameter space, the lightest eigenstate is essentially a wino of mass M_2 given in terms of $M_{1/2}$ by

$$M_2 = 0.82 M_{1/2}. \tag{17}$$

In the Higgs sector we can again make use of the fact that the non-singlet and singlet sectors are quasi-decoupled. The direct search for Higgs scalars thus proceeds as in the MSSM, and the present negative results do not impose more stringent constraints on $M_{1/2}$ than (16). (For large values of λ, without singlino LSP, the Higgs phenomenology of the (M+1)SSM could, however, differ substantially from the one of the MSSM [4].)

Since the scalar Higgs quasi-singlet state can possibly be produced in bino decays in the (M+1)SSM, its mass M_S will be of interest. From the tree level part of the Higgs potential one finds for small Yukawa couplings

$$M_S^2 \simeq \frac{1}{4}\sqrt{A_0^2 - 8m_0^2}\left(|A_0| + \sqrt{A_0^2 - 8m_0^2}\right), \tag{18}$$

hence

$$M_S \lesssim \frac{|A_0|}{\sqrt{2}}. \tag{19}$$

For later use we note that the coupling Higgs singlet–bino–singlino is proportional to λ^2, thus the production of the Higgs singlet state in bino decays will only occur for λ not too small.

To summarize, the parameter space of the (M+1)SSM with a singlino LSP is characterized by the universal gaugino mass $M_{1/2}$ being the dominant soft supersymmetry breaking term. Both A_0 and, consequently, m_0 are bounded from above in terms of $M_{1/2}$ by (11) and (7), respectively. The Yukawa couplings κ and λ also have upper limits of $O(10^{-2})$, and are possibly tiny.

The non-singlet sparticles (with sizable production cross sections) within the reach of LEP2 are: the second lightest neutralino, essentially a bino $\widetilde{B}$; the right handed sleptons $\widetilde{l}_\mathrm{R}$ with masses given by (14) and the lightest stau $\widetilde{\tau}_1$ which could be substantially lighter; sneutrinos with masses given by (15); and the lightest chargino with a mass given by (17). Note that, for a value of $M_{1/2}$ corresponding to a bino in the reach of LEP2, the bino is always lighter than these sparticles, with the possible exception of the lightest stau $\widetilde{\tau}_1$.

In the next section, we will discuss the different decays of these particles, and compare the respective final states to sparticle searches at LEP2. This will allow us to find out which parameter ranges of the (M+1)SSM have already been ruled out, and which require further study.

3 Topologies for sparticle searches at LEP2

3.1 Bino decays with a singlino LSP

Sparticle searches in the (M+1)SSM with a singlino LSP differ in several respects from sparticle searches in the MSSM. First, the presence of the singlino LSP usually gives rise to additional cascades in sparticle decays. For instance, pair production of binos is usually an observable process, whereas for an equivalent MSSM (with comparable soft supersymmetry breaking terms), the bino would correspond to the LSP, and this process would be invisible. Thus, areas in the soft SUSY breaking parameter space accessible at LEP2 are larger in the (M+1)SSM than in the MSSM, provided an adapted experimental analysis is done. Second, the decay of the NLSP (the bino or the lightest stau) into the singlino LSP is always proportional to a power of λ, which may be tiny. In this case (or if the singlino LSP happens to be close in mass to the NLSP, which is feasible in the (M+1)SSM with universal soft terms in contrast to the MSSM) the NLSP to LSP transition can be rather slow, leading to macroscopically displaced vertices.

In the following we can make use of the fact that the masses of most sparticles in the (M+1)SSM with a singlino LSP depend essentially on just one parameter, the universal gaugino mass $M_{1/2}$: For $M_{1/2}$ not too large ($M_{1/2} \lesssim 180\,\mathrm{GeV}$) $\widetilde{B}$, $\widetilde{l}_R$, $\widetilde{\nu}$ and $\widetilde{\chi}_1^\pm$ can be light enough for pair production to be kinematically allowed at LEP2, cf. the dependence of their mass on $M_{1/2}$ in Sect. 2. On the other hand, for $180\,\mathrm{GeV} \lesssim M_{1/2} \lesssim 220\,\mathrm{GeV}$, only $\widetilde{B}$ pair production is kinematically feasible (with the possible exception of staus).

Since all the sparticle decays in the (M+1)SSM with a singlino LSP proceed via the decay of the bino $\widetilde{B}$ into the singlino $\widetilde{S}$ (with the possible exception of the stau $\widetilde{\tau}_1$, see below), we will briefly discuss the possible final states of this transition, using the results of [7].

(a) $\widetilde{B} \to \widetilde{S}\nu\bar{\nu}$: This invisible process is mediated dominantly by sneutrino exchange. Since the sneutrino mass, as the mass of $\widetilde{B}$, is essentially fixed by $M_{1/2}$ (cf. (15)), the associated branching ratio varies in a predictable way with $M_{\widetilde{B}}$. It may become up to 90% for $M_{\widetilde{B}} \sim 30\,\mathrm{GeV}$, but decreases with $M_{\widetilde{B}}$ and is maximally 10% for $M_{\widetilde{B}} \gtrsim 65\,\mathrm{GeV}$.

(b) $\widetilde{B} \to \widetilde{S}l^+l^-$: This process is mediated dominantly by the exchange of a charged slepton in the s-channel. If the lightest stau $\widetilde{\tau}_1$ is considerably lighter than the sleptons of the first two generations, the percentage of taus among the charged leptons may well exceed 1/3. If $\widetilde{\tau}_1$ is lighter than $\widetilde{B}$, it is produced on shell, and the process becomes $\widetilde{B} \to \widetilde{\tau}_1\tau \to \widetilde{S}\tau^+\tau^-$. Hence we can have up to 100% taus

among the charged leptons and the branching ratio of this channel can become up to 100%.

(c) $\widetilde{B} \to \widetilde{S}S$: This two-body decay is kinematically allowed if both $\widetilde{S}$ and S are sufficiently light. (A light S is not excluded by Higgs searches at LEP1 [15,16], if its coupling to the Z is too small [4]). However, the coupling $\widetilde{B}\widetilde{S}S$ is proportional to λ^2, whereas the couplings appearing in the decays (a) and (b) are only of order $O(\lambda)$. Thus this decay can only be important for λ not too small. In [7], we found that its branching ratio can become up to 100% in a window $10^{-3} \lesssim \lambda \lesssim 10^{-2}$. Hence, its length of flight is never macroscopic. Of course, S will decay immediately into $b\bar{b}$ or $\tau^+\tau^-$, depending on its mass. (If the branching ratio $Br(\widetilde{B} \to \widetilde{S}S)$ is substantial, S is never lighter than $\sim 5\,\mathrm{GeV}$.) If the singlet is heavy enough, its $b\bar{b}$ decay gives rise to two jets with B mesons, which are easily detected with b-tagging. (However, if the singlet mass is just above the $b\bar{b}$ threshold – typically, if $m_\Upsilon < M_S \lesssim 15\,\mathrm{GeV}$ – S could decay hadronically without B mesons.) In any case, the hadronic system – or the $\tau^+\tau^-$ system – would have an invariant mass peaked at M_S, making this signature easy to search for.

(d) $\widetilde{B} \to \widetilde{S}\gamma$: This branching ratio may be important if the mass difference $\Delta M \equiv M_{\widetilde{B}} - M_{\widetilde{S}}$ is small ($\lesssim 5\,\mathrm{GeV}$).

Further possible final states like $\widetilde{B} \to \widetilde{S}q\bar{q}$ via Z exchange always have branching ratios below 10% and will not be considered here.

3.2 Constraints from MSSM-like selectron searches

Let us first consider the region in the parameter space where the invisible decay (a) of $\widetilde{B}$ dominates, which occurs for $M_{1/2} \lesssim 140\,\mathrm{GeV}$. Then, right handed selectrons $\widetilde{e}_R$ are light enough for being pair produced, and they decay as in the MSSM into an electron and a bino, which is invisible regardless of its life time. Results of searches for selectrons with MSSM-like decays have been published by Aleph [17], Delphi [18], L3 [19] and Opal [20][1]. Here, however, the analysis of the results differs from the situation in the MSSM in two respects.

First, for a given mass of the selectron, the mass difference $m_{\widetilde{e}_R} - M_{\widetilde{B}}$ is essentially known: for $m_{\widetilde{e}_R} = 65\,\mathrm{GeV}$, e.g., we have $m_{\widetilde{e}_R} - M_{\widetilde{B}} \sim 20$–$30\,\mathrm{GeV}$. It turns out that for the mass differences given in the present model, the experimental efficiencies are always $\gtrsim 50\%$.

On the other hand, the branching ratio associated with the invisible decay of $\widetilde{B}$ is never 100%. (Even for $M_{1/2} \lesssim 140\,\mathrm{GeV}$, $\widetilde{B}$ could still decay dominantly into $\widetilde{S}S$, if λ happens to be in the window $10^{-3} \lesssim \lambda \lesssim 10^{-2}$.) Thus, for each point in the parameter space, we have to calculate the expected number of MSSM-like events (two electrons and missing energy) taking the corresponding branching ratio into account.

[1] In this paper, we use the results from the LEP2 run at $s^{1/2} = 181$–$184\,\mathrm{GeV}$. For recent updates at $s^{1/2} = 189\,\mathrm{GeV}$, see [32]

The most detailed informations on the efficiencies, the numbers of background and observed events, as a function of $m_{\widetilde{e}_R}$ and $M_{\widetilde{B}}$, are given by Opal [20]. From these results, we find that points in the parameter space leading to $N \gtrsim 10$ expected events with two acoplanar electrons in the final state are excluded. This occurs in the region

$$M_{1/2} \lesssim 125\ \mathrm{GeV} \text{ or } M_{\widetilde{B}} \lesssim 43\,\mathrm{GeV}. \tag{20}$$

However, this region is not totally excluded by acoplanar electron searches: As mentioned above, $\widetilde{B}$ could still decay dominantly into $\widetilde{S}S$, if λ happens to be in the window $10^{-3} \lesssim \lambda \lesssim 10^{-2}$.

Further MSSM-like processes associated with two leptons and missing energy in the final state do not lead to additional constraints on the parameter space.

3.3 Higher multiplicity final states without displaced vertices

Next, we have to take into account visible $\widetilde{B}$ cascade decays, leading to events with a higher multiplicity. First we treat the case where all sparticle decays take place within at most 1 cm around the primary vertex, i.e. λ and ΔM not too small. The following pair production processes have to be considered:

$$\begin{aligned}
&\text{p.1: } e^+e^- \to \widetilde{B}\widetilde{B}, \\
&\text{p.2: } e^+e^- \to \widetilde{l}_R\widetilde{l}_R^* \ \to l^+\widetilde{B}l^-\widetilde{B}, \\
&\text{p.3: } e^+e^- \to \widetilde{\nu}\widetilde{\nu}^* \ \to \nu\widetilde{B}\bar{\nu}\widetilde{B}, \\
&\text{p.4: } e^+e^- \to \chi_1^+\chi_1^- \to l^+\widetilde{\nu}l'^-\bar{\widetilde{\nu}}^* \\
&\qquad\qquad\quad \to l^+\nu\widetilde{B}l'^-\bar{\nu}\widetilde{B}.
\end{aligned} \tag{21}$$

Taking the bino decays (a)–(c) in Sect. 3.1 into account, the possible final states are those listed in Table 1. (The radiative decay $\widetilde{B} \to \widetilde{S}\gamma$ will be discussed below.)

Let us first consider processes with four visible fermions and missing energy. The appropriate cascade decays of the binos leading to four charged fermions in the final state are: visible decays (b) $\widetilde{B} \to \widetilde{S}l^+l^-$ or (c) $\widetilde{B} \to \widetilde{S}S \to \widetilde{S}b\bar{b}$ or $\widetilde{S}\tau^+\tau^-$ for the two binos in p.1 and p.3 (the final states (i.1) and (i.3), i = 5 ... 9, in Table 1); one bino decaying invisibly through channel (a) $\widetilde{B} \to \widetilde{S}\nu\bar{\nu}$, the other decaying into l^+l^- or $b\bar{b}$ and missing energy through channels (b) or (c) for p.2 and p.4 (the final states (i.2) and (i.4), i = 2,3,4, in Table 1). In the case of the process p.4 we have used the fact that sneutrinos are always lighter than the lightest chargino in the (M+1)SSM with a singlino LSP; thus, the latter decays exclusively into an on-shell sneutrino and a charged lepton.

According to the discussion of the decay channel (b) above, the charged leptons $l^\pm$ in the final state may be the leptons of any generation. In the case of light staus, the percentage of taus among the charged leptons can become up to 100%. If the lightest stau $\widetilde{\tau}_1$ is the NLSP, p.2 and p.4 give six charged leptons plus missing energy in the final state. Only p.1 and p.3 lead to four charged leptons

Table 1. Visible final states after sparticle production in the case of microscopic vertices. (The $\widetilde{B}$ decay $\widetilde{B} \to \widetilde{S}S$ does not appear in the case of displaced vertices, see Sect. 3.4.) The leptons $\ell^+\ell^-$ can be leptons of any generation, including taus (which are possibly dominant). We have omitted photons from the decay $\widetilde{B} \to \widetilde{S}\gamma$, since these are always soft, see Sect. 3.3.

	Production process			
	p.1 $e^+e^- \to \widetilde{B}_1\widetilde{B}_2$	p.2 $e^+e^- \to \widetilde{l}_{\rm R}\widetilde{l}^*_{\rm R}$ $\to l^+\widetilde{B}_1 l^-\widetilde{B}_2$	p.3 $e^+e^- \to \widetilde{\nu}\widetilde{\nu}^*$ $\to \nu\widetilde{B}_1\bar{\nu}\widetilde{B}_2$	p.4 $e^+e^- \to \chi_1^+\chi_1^-$ $\to l^+\widetilde{\nu}l'^-\widetilde{\nu}^*$ $\to l^+\nu\widetilde{B}_1 l'^-\bar{\nu}\widetilde{B}_2$
Bino decays				
$\widetilde{B}_1 \to \widetilde{S}\nu\bar{\nu}$ $\widetilde{B}_2 \to \widetilde{S}\nu\bar{\nu}$	0 (1.1)	$l^+l^- + \not{E}_T$ (1.2)	0 (1.3)	$l^+l'^- + \not{E}_T$ (1.4)
$\widetilde{B}_1 \to \widetilde{S}\nu\bar{\nu}$ $\widetilde{B}_2 \to \widetilde{S}l^+l^-$	$l^+l^- + \not{E}_T$ (2.1)	$l^+l^-l^+l^- + \not{E}_T$ (2.2)	$l^+l^- + \not{E}_T$ (2.3)	$l^+l^-l^+l'^- + \not{E}_T$ (2.4)
$\widetilde{B}_1 \to \widetilde{S}\nu\bar{\nu}$ $\widetilde{B}_2 \to \widetilde{S}S \to \widetilde{S}b\bar{b}$	$b\bar{b} + \not{E}_T$ (3.1)	$l^+l^-b\bar{b} + \not{E}_T$ (3.2)	$b\bar{b} + \not{E}_T$ (3.3)	$l^+l'^-b\bar{b} + \not{E}_T$ (3.4)
$\widetilde{B}_1 \to \widetilde{S}\nu\bar{\nu}$ $\widetilde{B}_2 \to \widetilde{S}S \to \widetilde{S}\tau^+\tau^-$	$\tau^+\tau^- + \not{E}_T$ (4.1)	$l^+l^-\tau^+\tau^- + \not{E}_T$ (4.2)	$\tau^+\tau^- + \not{E}_T$ (4.3)	$l^+l'^-\tau^+\tau^- + \not{E}_T$ (4.4)
$\widetilde{B}_1 \to \widetilde{S}l^+l^-$ $\widetilde{B}_2 \to \widetilde{S}l^+l^-$	$l^+l^-l^+l^- + \not{E}_T$ (5.1)	$l^+l^-l^+l^-l^+l^- + \not{E}_T$ (5.2)	$l^+l^-l^+l^- + \not{E}_T$ (5.3)	$l^+l^-l^+l^-l^+l'^- + \not{E}_T$ (5.4)
$\widetilde{B}_1 \to \widetilde{S}l^+l^-$ $\widetilde{B}_2 \to \widetilde{S}S \to \widetilde{S}b\bar{b}$	$l^+l^-b\bar{b} + \not{E}_T$ (6.1)	$l^+l^-l^+l^-b\bar{b} + \not{E}_T$ (6.2)	$l^+l^-b\bar{b} + \not{E}_T$ (6.3)	$l^+l^-b\bar{b}l^+l'^- + \not{E}_T$ (6.4)
$\widetilde{B}_1 \to \widetilde{S}l^+l^-$ $\widetilde{B}_2 \to \widetilde{S}S \to \widetilde{S}\tau^+\tau^-$	$l^+l^-\tau^+\tau^- + \not{E}_T$ (7.1)	$l^+l^-l^+l^-\tau^+\tau^- + \not{E}_T$ (7.2)	$l^+l^-\tau^+\tau^- + \not{E}_T$ (7.3)	$l^+l^-\tau^+\tau^-l^+l'^- + \not{E}_T$ (7.4)
$\widetilde{B}_1 \to \widetilde{S}S \to \widetilde{S}b\bar{b}$ $\widetilde{B}_2 \to \widetilde{S}S \to \widetilde{S}b\bar{b}$	$b\bar{b}b\bar{b} + \not{E}_T$ (8.1)	$l^+l^-b\bar{b}b\bar{b} + \not{E}_T$ (8.2)	$b\bar{b}b\bar{b} + \not{E}_T$ (8.3)	$b\bar{b}b\bar{b}l^+l'^- + \not{E}_T$ (8.4)
$\widetilde{B}_1 \to \widetilde{S}S \to \widetilde{S}\tau^+\tau^-$ $\widetilde{B}_2 \to \widetilde{S}S \to \widetilde{S}\tau^+\tau^-$	$\tau^+\tau^-\tau^+\tau^- + \not{E}_T$ (9.1)	$l^+l^-\tau^+\tau^-\tau^+\tau^- + \not{E}_T$ (9.2)	$\tau^+\tau^-\tau^+\tau^- + \not{E}_T$ (9.3)	$\tau^+\tau^-\tau^+\tau^-l^+l'^- + \not{E}_T$ (9.4)

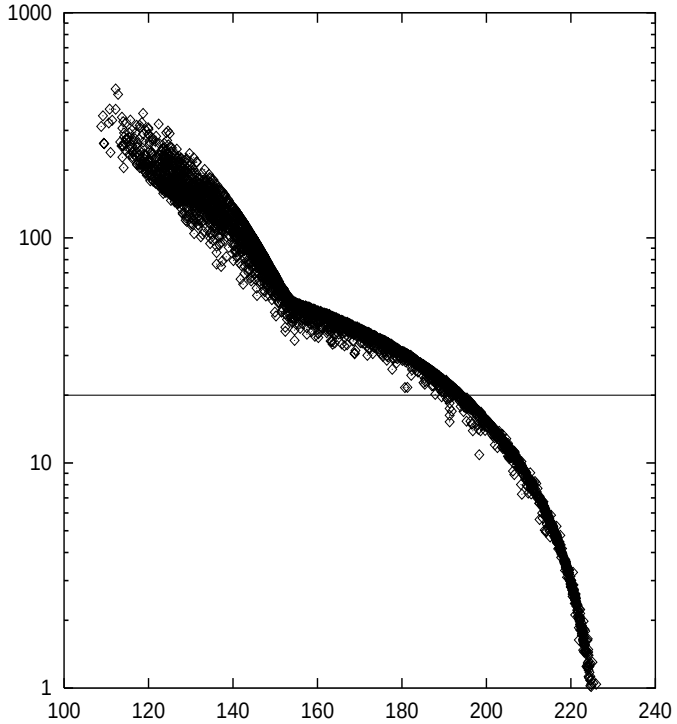

Fig. 1. Number of four charged fermion events expected from $\widetilde{B}$, $\widetilde{e}_{\rm R}$, $\widetilde{\tau}_1$, $\chi_1^{\pm}$ pair production as a function of $M_{1/2}$.

(taus) plus missing energy, since, in this case, the only decay channel for the bino is $\widetilde{B} \to \tau\widetilde{\tau}_1 \to \widetilde{S}\tau^+\tau^-$.

Thus, the final states of interest are $l^+l^-l^+l^-$, $l^+l^-b\bar{b}$ and $b\bar{b}b\bar{b}$ plus missing energy. Since the bs can arise solely from the decay (c) $\widetilde{B} \to \widetilde{S}S \to \widetilde{S}b\bar{b}$, the invariant mass of a $b\bar{b}$ system would always be peaked at M_S, cf. the discussion above. However, for a given value of $M_{1/2}$, we cannot predict the different branching ratios of $\widetilde{B}$ (λ may or may not be in the window where the decay into $\widetilde{S}S$ is dominant), hence we cannot predict the ratios of the different final states associated to a given process in (21). On the other hand, for a given value of $M_{1/2}$ we know, with small errors, the masses $M_{\widetilde{B}}$, $m_{\widetilde{l}_R}$, $m_{\widetilde{\nu}}$ and $M_{\chi_1^{\pm}}$ and the corresponding production cross sections. For each point in the parameter space obtained from the scanning described in the previous section, we have numerically calculated the production cross sections of the proceses p.1-4, taking into account possible interference terms between the s-, t- and u-channels [13], for e^+e^- collisions at 183 GeV c.m. energy. In Fig. 1 we show, for each point in the parameter space, the total number of events with four charged fermions plus missing energy in the final state as a function of $M_{1/2}$, assuming an integrated luminosity of $55\,{\rm pb}^{-1}$. We have already removed those points in the parameter space where $\widetilde{B}$ decays dominantly invisibly through channel (a), and which are excluded by the negative results of selectron searches in the MSSM; see the discussion above. Moreover, we have not shown the points where $\widetilde{B}$ decays dominantly into channel (d) $\widetilde{B} \to \widetilde{S}\gamma$ which will be discussed separately below.

In Fig. 1 we observe a large number of events for $M_{1/2} \lesssim 150\,{\rm GeV}$, which are due to process p.3: If kinematically allowed, its cross section is typically larger than the ones of p.1, p.2 or p.4. For $M_{1/2} \gtrsim 150\,{\rm GeV}$, on the other hand, the number of events is essentially given by the number of $\widetilde{B}$ being pair produced (p.1).

Events with four charged fermions plus missing energy in the final state have been searched at LEP2. The underlying processes were assumed to be: $\widetilde{t}_1$ pair production with $\widetilde{t}_1 \to bl\widetilde{\nu}$ [21,18], and heavy neutralinos decaying via the Multi Lepton channel [22] in the MSSM; lightest neutralino pair production in models with gauge mediated supersymmetry breaking (i.e. a gravitino LSP) and a stau NLSP [24]; or any sparticle pair production process in the context of models with R-parity violation [26].

Standard backgrounds with four charged fermions and missing energy are small and typically, after imposing appropriate cuts, the number of background events in a given channel vary from 0 to 4, with a comparable number of observed events. No excess has been observed. The given efficiencies vary roughly between 20% and 60%, depending, e.g. in $\not{R}_p$ models, on the mass of the unstable (intermediate) neutralino.

Of course we cannot apply these efficiencies to the processes listed in (21). The kinematics of these processes is often very different from the kinematics of the assumed underlying processes, and also various branching ratios into different final states would have to be considered. (In particular in the case of small mass difference ΔM the efficiencies for the processes p.1–p.4 could be quite low.)

From Fig. 1 we can only deduce which range of values for $M_{1/2}$ could be excluded. For instance, assuming a minimal efficiency of 20% for all processes listed in (21), and assuming a total number of four expected events excluded, we would conclude that the total number of actual events has to be smaller than 20 implying a lower limit on $M_{1/2}$ or $M_{\widetilde{B}}$ of

$$M_{1/2} \gtrsim 190\ {\rm GeV} \text{ or } M_{\widetilde{B}} \gtrsim 75\,{\rm GeV}. \qquad (22)$$

(In Fig. 1 we have indicated this example by a horizontal line.)

Events with six charged fermions in the final state can also appear in slepton or chargino pair production (processes p.2 and p.4, the final states (i.2) and (i.4), i = 5 ... 9, in Table 1). However, the bino is always lighter than these sparticles (with the possible exception of the stau, see below), and the regime in the parameter space covered by $\widetilde{B}$ pair production (and four charged fermions in the final state) is always larger.

Next, we briefly comment on the case (d) where $\widetilde{B}$ decays dominantly into $\widetilde{S}\gamma$. Note that this branching ratio can only be important for a small mass difference $\Delta M = M_{\widetilde{B}} - M_{\widetilde{S}} \lesssim 5\,{\rm GeV}$. This decay could lead to final states with just two isolated photons and missing energy (via p.1 and p.3) or two leptons plus two isolated photons and missing energy (via p.2 and p.4). In the first case , however, detection efficiencies are always very small due to the small mass difference ΔM [27–30]. Final states

of the form $l^+l^-\gamma\gamma + \not{E}_T$ have been searched in [17,25, 23], where gauge mediated supersymmetry breaking (i.e. a gravitino LSP) was assumed. Again, however, the efficiencies corresponding to the assumed underlying process do not apply to the present case due to the small value of ΔM. On the other hand, if the photons are soft enough to be accepted as low energy neutral clusters in acoplanar lepton searches, the MSSM constraint on the selectron mass $m_{\widetilde{e}_R} \lesssim 80\,\mathrm{GeV}$ [17–20] applies, leading to a lower limit on $M_{1/2}$ ($M_{\widetilde{B}}$) of

$$M_{1/2} \gtrsim 175\,\mathrm{GeV} \text{ or } M_{\widetilde{B}} \gtrsim 67\,\mathrm{GeV}. \quad (23)$$

Clearly this case requires a dedicated analysis depending on the various detectors.

3.4 Final states with neutral displaced vertices

Up to now, we have considered the case of a microscopic life time of $\widetilde{B}$. For a small Yukawa coupling λ or a small ΔM, however, the length of flight of $\widetilde{B}$ can become large, leading to macroscopically displaced vertices [7]. Let us first remark that, in this case, the decay channel (c) $\widetilde{B} \to \widetilde{S}S$ is impossible: If the decay length of $\widetilde{B}$ is large, either λ is very small and thus outside the window $10^{-3} \lesssim \lambda \lesssim 10^{-2}$, or ΔM is small so that the quasi-singlet Higgs scalar S can no longer be produced on shell. Furthermore, the region of the parameter space where the invisible decay channel (a) $\widetilde{B} \to \widetilde{S}\nu\bar{\nu}$ dominates has already been treated above, regardless of the $\widetilde{B}$ life time. In this case, selectron pair production (p.2 in (21)) looks like in the MSSM. Taking into account the dependence of this branching ratio on $M_{1/2}$, the corresponding efficiencies and numbers of background/observed events, one finds that the region (20) can be completely excluded. (As a matter of fact, since the decay channel (c) plays no role for displaced vertices, the bino decays always invisibly in this region of the parameter space.) Therefore, the remaining decay channels for a bino with $M_{\widetilde{B}} \gtrsim 43\,\mathrm{GeV}$ are (b) $\widetilde{B} \to \widetilde{S}l^+l^-$ and (d) $\widetilde{B} \to \widetilde{S}\gamma$. In the situation of a macroscopic length of flight, the cases of a $\widetilde{B}$ decay inside or outside the detector have to be treated separately.

If $\widetilde{B}$ decays inside the detector ("mesoscopic" decay length: $1\,\mathrm{cm} \lesssim l_{\widetilde{B}} \lesssim 3\,\mathrm{m}$, where $l_{\widetilde{B}}$ denotes the decay length in the laboratory system), the following topologies are possible.

• The processes p.2 (charged slepton pair production) and p.4 (chargino pair production) give rise to two acoplanar leptons from the primary vertex plus neutral displaced clusters (lepton pairs or photons) due to delayed $\widetilde{B}$ decay. Searches for events with neutral clusters have not been published up to now, due to vetos against such clusters in order to remove the background from radiative events [17–20]. However, for small values of ΔM (mainly when $\widetilde{B}$ decays dominantly into $\widetilde{S}\gamma$) such neutral clusters could be soft enough not to be vetoed (cf. the discussion above on photons in the final state). In this case, the limit on the selectron mass in the MSSM leads to the lower limit (23) on $M_{1/2}$ ($M_{\widetilde{B}}$).

• The process p.1 (bino pair production) leads to events with just neutral displaced vertices and no activity at the primary vertex. Since, in this case, $\widetilde{B}$ is the lightest visible particle of the model, this process would allow one to test a larger region in the parameter space than the processes p.2 and p.4 discussed above. The expected event rates are as in Fig. 1 for $M_{1/2} \gtrsim 150\,\mathrm{GeV}$. If ΔM is not too small, the decay product of $\widetilde{B}$ would be charged leptons with at least 33% taus. Clearly this topology is the most difficult one to detect (since triggers around the primary vertex will not be active[2]), and no constraints on such processes have been published. On the other hand, for small ΔM, the photonic decay channel (d) dominates. Searches have been performed within the MSSM for χ_2^0 pair production followed by a delayed $\chi_2^0 \to \chi_1^0\gamma$ decay [28]. However, the efficiency for small mass differences is tiny and this channel cannot be used. In the region of the parameter space where this decay channel dominates, the relevant topology is two acoplanar electrons arising from selectron pair production, the photons being soft enough for being accepted as extra neutral clusters in this search (cf. above).

If $\widetilde{B}$ decays outside the detector ("macroscopic" decay length: $l_{\widetilde{B}} > 3\,\mathrm{m}$), the situation in the (M+1)SSM with a singlino LSP is clearly the same as in the corresponding MSSM with $\widetilde{B}$ being the true LSP. In particular, the MSSM constraint on the selectron mass can be applied directly with the additional benefit that $m_{\widetilde{e}_R} - M_{\widetilde{B}}$ is known in terms of $m_{\widetilde{e}_R}$. Hence, the lower limit on $M_{1/2}$ ($M_{\widetilde{B}}$) is given by (23).

The present constraints for the various ranges of $M_{1/2}$ (or $M_{\widetilde{B}}$) and the various $\widetilde{B}$ life times are summarized in Fig. 2. On the bottom horizontal line of Fig. 2, we plot $M_{1/2}$ in the range of interest, and on the top horizontal line we indicate the corresponding values of $M_{\widetilde{B}}$ (with $\lesssim 5\,\mathrm{GeV}$ accuracy). On the vertical axis, we plot the $\widetilde{B}$ decay length in the laboratory system. In this plane we have indicated in grey those regions (for to $l_{\widetilde{B}} > 1\,\mathrm{cm}$), which are excluded by negative results from acoplanar electron searches. For $l_{\widetilde{B}} < 1\,\mathrm{cm}$ the total number of events with four charged fermions and missing energy in the final state exceeds 20 in the striped region.

As mentioned above, in the (M+1)SSM with a singlino LSP, the NLSP could possibly be a stau. Then, limits from MSSM stau searches can be applied. Again, if λ (or $m_{\widetilde{\tau}_1} - M_{\widetilde{S}}$) is sufficiently small, the $\widetilde{\tau}_1$ life time can become large and may give rise to displaced vertices. Medium- or long-lived charged scalars have been searched at LEP2 [17,31,24], and the corresponding constraints can also be applied here. However, the lower limit on stau masses does not correspond to a definite region in the $(l_{\widetilde{B}}, M_{1/2})$ plane of Fig. 2 which is or is not excluded, since even for large values of $M_{1/2}$, $m_{\widetilde{\tau}_1}$ can still be relatively small. (Of course, $\widetilde{B}$ pair production can still be used, where now the

[2] One could use, however, an initial state radiative photon to trigger the event.

$\widetilde{B}$ decays always through the cascade $\widetilde{B} \to \widetilde{\tau}_1\tau \to \widetilde{S}\tau\tau$. Hence, the $\widetilde{B}$ life time is always very small. If, in addition, the stau life time is also small, the processes p.1 and p.3 in (21) give rise to the same topology as in the case of a bino NLSP: four charged leptons (taus) plus missing energy. As discussed before, this case is included in Fig. 1.)

4 Summary and outlook

We have seen that the final state topologies of the (M+1)SSM with a singlino LSP can differ considerably from the MSSM, due to the additional $\widetilde{B} \to \widetilde{S}X$ cascade. Since these topologies can be the first sign of sparticle production at LEP2, it is very important to identify them carefully.

In the present paper we have identified these topologies, and studied the parameter space of the model in order to check whether there are regions not excluded by negative results from MSSM-like sparticles searches, though accessible at LEP2 (i.e. with a reasonable expected number of events).

Indeed we found several such regions, and the associate topologies have been listed in Table 1: First, we can have four charged fermions of various kinds and missing energy in the final state. Such final states have been looked for in the context of the MSSM, e.g. in stop and neutralino searches, or in models with R-parity violation. However, the corresponding efficiencies within the present model are not known up to now.

In Fig. 1 we have shown the total number of events which can be expected within the present model as a function of $M_{1/2}$ (which can be translated into $M_{\widetilde{B}}$ using (10)). Clearly, assuming a small but non-vanishing efficiency for the topologies of the present model, the region $M_{1/2} \lesssim 140\,\mathrm{GeV}$, corresponding to $> O(10^2)$ total events, could already be excluded from searches for four charged fermions. Of particular interest is, however, the region $M_{1/2} \gtrsim 150\,\mathrm{GeV}$ where only $\widetilde{B}$ pair production contributes to this topology; this process allows one to test the largest region in the parameter space. With the corresponding efficiencies at hand one could expect, e.g., a sensitivity to a total number of $N > 20$ of four charged fermion events plus missing energy, which would allow one to test the region up to $M_{1/2} \lesssim 190\,\mathrm{GeV}$ (or $M_{\widetilde{B}} \lesssim 75\,\mathrm{GeV}$) as indicated by the horizontal line in Fig. 1, or the striped region in Fig. 2. Note that final states with six charged fermions can only appear after slepton or chargino pair production (processes p.2 and p.4 in (21)). The accessible parameter space is thus smaller than the one covered by $\widetilde{B}$ pair production.

If the decay length of $\widetilde{B}$ is mesoscopic ($1\,\mathrm{cm} \lesssim l_{\widetilde{B}} \lesssim 3\,\mathrm{m}$) and $\widetilde{B}$ decays visibly, new topologies appear: either two leptons at the primary vertex (from slepton or chargino pair production) plus neutral displaced clusters due to the delayed $\widetilde{B}$ decay, or just neutral displaced clusters from $\widetilde{B}$ pair production. The latter process is even more promising since it allows to test a larger region in the parameter space, although it is certainly the most difficult to trigger on.

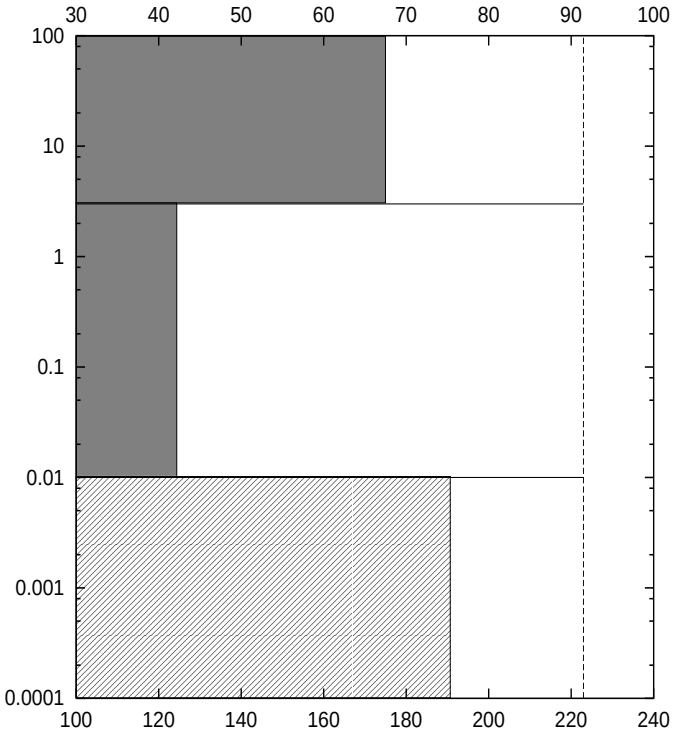

Fig. 2. Regions in the plane $l_{\widetilde{B}}$ (in the laboratory system) vs. $M_{1/2}$, which are excluded due to negative results from searches for acoplanar electrons at LEP2, are indicated in grey. (On the top horizontal line we indicate the corresponding values of $M_{\widetilde{B}}$, with $\lesssim 5\,\mathrm{GeV}$ accuracy). The remaining regions still have to be explored. In the striped region, for $l_{\widetilde{B}} < 1\,\mathrm{cm}$, the total number of events with four charged fermions and missing energy in the final state exceeds 20. The vertical dashed line indicates the kinematic limit for $\widetilde{B}$ pair production at LEP2 with $s^{1/2} = 183\,\mathrm{GeV}$.

Again, the total number of expected events, as a function of $M_{1/2}$ (or $M_{\widetilde{B}}$), can be deduced from Fig. 1. Now, however, the estimation of the corresponding efficiencies is much more delicate. On the other hand, the decay channel (c) $\widetilde{B} \to \widetilde{S}S$ never appears in this range of the decay length $l_{\widetilde{B}}$, and the number of possible final states is reduced. (Now, the region $M_{1/2} \lesssim 125\,\mathrm{GeV}$ can already be excluded: Here the bino decays nearly always invisibly, and the negative results from acoplanar leptons plus missing energy searches – associated with the process p.2 in (21) – can be applied. This is indicated in Fig. 2 in the form of the grey region for $1\,\mathrm{cm} \lesssim l_{\widetilde{B}} \lesssim 3\,\mathrm{m}$.)

Herewith we would like to encourage searches for these unconventional topologies, in order to cover the entire parameter space of the (M+1)SSM with a singlino LSP. If no excesses are observed at LEP2, we will have to turn to larger c.m. energies at the Tevatron (Run II), the LHC or – hopefully – the NLC. Again, the (M+1)SSM with a singlino LSP predicts unconventional signals for these machines, like additional decay cascades (as compared to the MSSM) or displaced vertices. The details of these topolo-

gies and the expected event rates as a function of the parameters of the (M+1)SSM will have to be considered in the near future.

Acknowledgements. It is a pleasure to thank L. Duflot for helpful comments. Many useful discussions in the framework of the French workshop "GDR Supersymétrie" are also acknowledged.

References

1. P. Fayet, Nucl. Phys. B **90**, 104 (1975); H.P. Nilles, M. Srednicki, D. Wyler, Phys. Lett. B **120**, 346 (1983); J. Ellis, J.F. Gunion, H.E. Haber, L. Roszkowski, F. Zwirner, Phys. Rev. D **39**, 844 (1989); L. Durand, J.L. Lopez, Phys. Lett. B **217**, 463 (1989); M. Drees, Int. J. Mod. Phys. A **4**, 3635 (1989)
2. J.P. Derendinger, C.A. Savoy, Nucl. Phys. B **237**, 307 (1984)
3. L.E. Ibañez, C. Lopez, Nucl. Phys. B **233**, 511 (1984); C. Kounnas, A.B. Lahanas, D.V. Nanopoulos, M. Quirós, Nucl. Phys. B **236**, 438 (1984); A. Bouquet, J. Kaplan, C.A. Savoy, Nucl. Phys. B **262**, 299 (1985); P. Brax, C.A. Savoy, Nucl. Phys. B **447**, 227 (1995)
4. U. Ellwanger, Phys. Lett. B **303**, 271 (1993); U. Ellwanger, M. Rausch de Traubenberg, C.A. Savoy, Z. Phys. C **67**, 665 (1995); T. Elliott, S.F. King, P.L. White, Phys. Rev. D **49**, 2435 (1994)
5. U. Ellwanger, M. Rausch de Traubenberg, C.A. Savoy, Phys. Lett. B **315**, 331 (1993); S.F. King, P.L. White, Phys. Rev. D **52**, 4183 (1995)
6. U. Ellwanger, M. Rausch de Traubenberg, C.A. Savoy, Nucl. Phys. B **492**, 21 (1997)
7. U. Ellwanger, C. Hugonie, Eur. Phys. J. C **5**, 723 (1998)
8. S.A. Abel, S. Sarkar, P.L. White, Nucl. Phys. B **454**, 663 (1995); S.A. Abel, Nucl. Phys. B 480 (1996) 55; hep-ph 9603301
9. F. Franke, H. Fraas, Z. Phys. C **72**, 309 (1996)
10. A. Stephan, Phys. Rev. D 58 (1998); Phys. Lett. B **411**, 97 (1997)
11. A. de Gouvea, A. Friedland, H. Murayama, Phys. Rev. D **59**, 095008 (1999)
12. H.E. Haber, G.L. Kane, Phys. Rep. **117**, 75 (1985)
13. H. Baer, A. Bartl, D. Karatas, W. Majerotto, X. Tata, Int. J. Mod. Phys. A **4**, 4111 (1989) and references therein
14. J.F. Grivaz, hep-ph/9709505 (to appear in Perspectives on Supersymmetry, edited by G.L. Kane (World Scientific Publishing, Singapore)
15. Aleph collab., Phys. Lett. B **313**, 312 (1993); Delphi collab., Nucl. Phys. B **373**, 3 (1992); L3 collab., Z. Phys. C **57**, 355 (1993); Opal collab., Z. Phys. C **64**, 1 (1994)
16. Aleph collab., CERN-EP/98-145 (submitted to Phys. Lett. B); Delphi collab., DELPHI/98-95; L3 collab., Phys. Lett. B **436**, 389 (1998); Opal collab., CERN-EP/98-173 (to appear in Eur. Phys. J. C)
17. Aleph collab., Phys. Lett. B **433**, 176 (1998)
18. Delphi collab., DELPHI/98-92
19. L3 collab., L3-N/2287
20. Opal collab., CERN-EP/98-122 (submitted to Eur. Phys. J. C)
21. Aleph collab., CERN-EP/98-076 (submitted to Phys. Lett. B); L3 collab., CERN-EP/98-135 (submitted to Phys. Lett. B); Opal collab., CERN-EP/98-107 (to appear in Eur. Phys. J. C)
22. Aleph collab., ALEPH/98-071
23. Delphi collab., CERN-EP/98-176 (to appear in Phys. Lett. B)
24. Delphi collab., CERN-EP/98-170 (to appear in Eur. Phys. J. C)
25. Opal collab., OPAL-PN/332
26. Aleph collab., ALEPH/98-027; Delphi collab., DELPHI/98-138; L3 collab., L3-N/2291; Opal collab., OPAL-PN/356 and OPAL-PN/359 (submitted to Eur. Phys. J. C)
27. Aleph collab., Phys. Lett. B **429**, 201 (1998)
28. Delphi collab., CERN-EP/98-142 (to appear in Eur. Phys. J. C)
29. L3 collab., CERN-EP/98-150 (to appear in Phys. Lett. B)
30. Opal collab., CERN EP/98-143 (to appear in Eur. Phys. J. C)
31. Aleph collab., Phys. Lett. B **405**, 379 (1997); Delphi collab., CERN-EP/98-171 (to appear in Phys. Lett. B); Opal collab., Phys. Lett. B **433**, 195 (1998)
32. Aleph collab., ALEPH/98-072; Delphi collab., DELPHI/98-137; L3 collab., L3-N/2309; Opal collab., OPAL-PN/362